A novel grating lobes suppression method of sparse arrays for acoustic source locating

Yilin Wang[123], Tian Lan[3], Yun Yu[3], Nan Zou[123], Guolong Liang[123]

1. Acoustic Science and Technology Laboratory, Harbin Engineering University, Harbin, China.
2. Key Laboratory of Marine Information Acquisition and Security (Harbin Engineering University), Ministry of Industry and Information Technology, Harbin, China.
3. College of Underwater Acoustic Engineering, Harbin Engineering University, Harbin, China.
Corresponding author and Speaker: Nan Zou (zounan@hrbeu.edu.cn)

Abstract — Due to the large size of fiber hydrophone, only sparse configuration can be applied to high frequency optical fiber arrays. Ineluctably, the grating lobes are generated and the orientation estimation fuzzy problem is caused. To solve this problem, a combined sparse array structure is designed and a grating lobes suppression technique is proposed. This method is based on three co-prime sparse optical fiber sensor arrays, which collect the incident signal of targets and then process it comprehensively. Compared with the traditional uniform array, the number of elements is reduced, which has a strong practical engineering value. The simulation results show that the proposed method can effectively suppress the grating lobes and estimate the target's orientation accurately.

***Index Terms*—Coprime sensor arrays, high frequency signal, array processing.**

I. INTRODUCTION

Array signal processing utilizes sensor arrays to sample the signal which can be calculated and processed, then the useful information is extracted. There are two basic tasks in array signal processing, one is beamforming and the other is spatial spectrum estimation. With the development of array signal processing theory, algorithms such as CBF, MVDR, MUSIC, ESPRIT, max-likelihood method and sparse reconstruction have appeared. Most of the above algorithms are based on uniform array and the spacing of the inner elements must be less than or equal to half wavelength of the impinging signal, resulting in that the aperture is restricted by the number of elements. For uniform array, the number of elements must be increased to obtain high resolution, which leads to high hardware cost and difficult array design.

Optical fiber hydrophones have many advantages like high sensitivity, low transmission loss, reduced crosstalk over the traditional ones. What's more, the volume and weight of the arrays are greatly reduced. Thus, optical fiber arrays can be arranged on ships, submarines, miniaturization surface vehicle, unmanned underwater platform in order to establish a large-scale and omnibearing 3D acoustic sensor network, which improves the ability to the real-time monitoring of underwater environment and ensures access to information advantage in anti-submarine warfare. However, due to the unique structure of fiber optic hydrophones, it's hard to meet the requirement that the spacing of elements should be less than or equal to half wavelength when high frequency impinging signal is detected and estimated.

Aiming at the above problems, a new sparse array structure is designed. Different from uniform array, the spacing of elements can exceed the half wavelength limit, which can obtain larger aperture. Therefore, when the optical fiber hydrophones are assembled for high-frequency signal detection and localization, the design has high practical significance, which will save hardware resource and effectively promote the application of related signal processing algorithm.

II. SIGNAL MODEL

This paper aims to solve the problem of angle ambiguity caused by the detection of high frequency signals and the problem of waste caused by the redundancy of array elements. So, a high frequency signal detection system based on optical fiber hydrophones is designed. The design steps are as follows:

Firstly, the array structure of optical fiber sensor array is designed, including three sub-arrays 1, 2 and 3 in sequence. The sub arrays are uniform linear arrays, and the element spacing is coprime between different arrays. Secondly, for each sub-array, beamforming and DOA estimation are carried out. Thirdly, based on the designed array, the information in the beam domain of the three sub-arrays is comprehensively processed by utilizing the characteristics of coprime spacing between the elements of each sub array, which suppresses the

grating lobes. The spatial spectrum is obtained and the azimuth of the target is estimated.

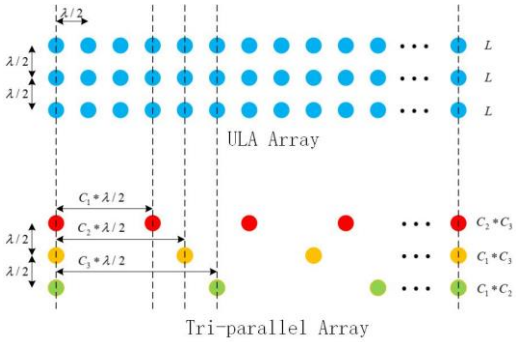

Fig. 1. Tri-parallel Array Configuration

As is shown in Fig.1, the coprime factors of the three subarrays are respectively C_1, C_2 and C_3 ($C_1, C_2, C_3 \geq 2$), and the spacing of the sub-arrays is $\lambda/2$. The elements number of sub-array 1 is $M_1 = C_2 * C_3$ and the spacing is $C_1 * \lambda/2$; The elements number of sub-array 2 is $M_2 = C_1 * C_3$ and the spacing is $C_2 * \lambda/2$; The elements number of sub-array 3 is $M_3 = C_1 * C_2$ and the spacing is $C_3 * \lambda/2$; the wavelength of the impinging signal is λ.

A. Conventional Beamforming

As is shown in Fig.2, the scanning range of the conventional beam forming is:

Azimuth angle: $\theta \in (0°, 180°)$;

Pitch angle: $\varphi \in (-90°, 90°)$;

Direction of incident signal (θ_0, φ_0).

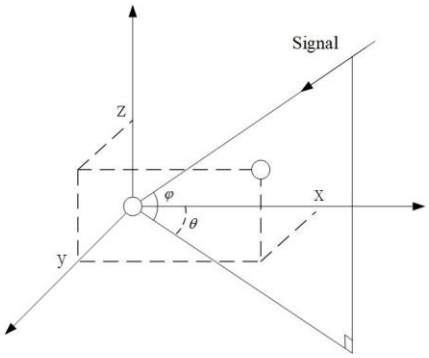

Fig. 2. Signal Model

For each subarray i, $i = 1,2,3$, the signal received at a certain time $x_{i(1\sim M_i)}(t)$ can be arranged into a column vector:

$$\begin{bmatrix} x_1(t) \\ x_2(t) \\ \vdots \\ x_{M_i}(t) \end{bmatrix} = \begin{bmatrix} e^{-j\omega_0\tau_{11}} & e^{-j\omega_0\tau_{12}} & \cdots & e^{-j\omega_0\tau_{1N}} \\ e^{-j\omega_0\tau_{21}} & e^{-j\omega_0\tau_{22}} & \cdots & e^{-j\omega_0\tau_{2N}} \\ \vdots & \vdots & & \vdots \\ e^{-j\omega_0\tau_{M_i1}} & e^{-j\omega_0\tau_{M_i2}} & \cdots & e^{-j\omega_0\tau_{M_iN}} \end{bmatrix} \begin{bmatrix} s_1(t) \\ s_2(t) \\ \vdots \\ s_N(t) \end{bmatrix} + \begin{bmatrix} n_1(t) \\ n_2(t) \\ \vdots \\ n_{M_i}(t) \end{bmatrix} \quad (1)$$

where the number of incident signals is N and the frequency of impinging signal is ω_0. $s_{i(1\sim N)}(t)$ represents the complex envelope of signal and $n_{i(1\sim M_i)}(t)$ represents the noise. The time delay between elements and the reference element is $\tau_{i(1\sim M_i)N}$.

The above signal column vector can be expressed as a vector as follows:

$$\mathbf{X}_i(t) = \mathbf{A}_i\mathbf{S}_i(t) + \mathbf{N}_i(t), i = 1,2,3 \quad (2)$$

where, $\mathbf{X}_i(t) = [x_{i1}(t), x_{i2}(t), ..., x_{iM_i}(t)]^T$;

$\mathbf{N}_i(t) = [n_{i1}(t), n_{i2}(t), ..., n_{iM_i}(t)]^T$;

and $\mathbf{S}_i(t) = [s_{i1}(t), s_{i2}(t), ..., s_{iN}(t)]^T$;

$\mathbf{A}_i$ is array manifold of each sub-array, which can be denoted as:

$$\boldsymbol{A}_i = \left[\boldsymbol{a}_{i1}(\omega_0) \quad \boldsymbol{a}_{i2}(\omega_0) \quad \cdots \quad \boldsymbol{a}_{iN}(\omega_0)\right], i = 1,2,3 \quad (3)$$

where the Steering vector can be expressed as,

$$\boldsymbol{a}_i(\omega_0) = \begin{bmatrix} \exp(-j\omega_0\tau_{i1k}) \\ \exp(-j\omega_0\tau_{i2k}) \\ \vdots \\ \exp(-j\omega_0\tau_{iM_ik}) \end{bmatrix}, i = 1,2,3, k = 1,2,...,N \quad (4)$$

The 1st array element of the second sub-array is located on the point $(0,0,0)$, the position of the other elements in space is (x,y,z), and the time delay derived from geometric relations between two arrays is:

$$\tau = \frac{1}{c}(x\cos\theta\cos\varphi + y\sin\theta\cos\varphi + z\sin\varphi) \quad (5)$$

Let the weight of the sub-array i be w_i and the weighted output is:

$$y_i(\theta,\varphi) = \boldsymbol{w}_i^H(\theta,\varphi)\boldsymbol{X}_i, \quad i = 1,2,3 \quad (6)$$

Conventional beam forming (CBF) is carried out and make $\boldsymbol{w}_i = \boldsymbol{a}_i(\theta_0, \varphi_0)$. The covariance matrix is expressed as $\boldsymbol{R}_{xi}$ and searched within the scanning range to obtain the spatial power spectrum, that is,

$$P_i(\theta,\varphi) = \boldsymbol{a}_i^H(\theta,\varphi)\boldsymbol{R}_{ix}\boldsymbol{a}_i(\theta,\varphi), i = 1,2,3 \quad (7)$$

In space estimation, snapshots p is often used to instead $\boldsymbol{R}_{xi}$, i.e.,

$$\boldsymbol{R}_{\text{ix}} = \frac{1}{p}\sum_{n=1}^{p}\left[\boldsymbol{X}_i(n)\boldsymbol{X}_i^H(n)\right], i=1,2,3 \tag{8}$$

The obtained $P_1(\theta,\varphi)$, $P_2(\theta,\varphi)$ and $P_3(\theta,\varphi)$ are the basic orientation information obtained from the three sub-arrays respectively.

Due to the spatial undersampling, the spatial spectrum obtained by the conventional beamforming scanning of each sub-array is affected by gating lobes, which seriously affect the quality of signal azimuth estimation.

B. Minimum Variance Distortionless Response Beamforming

Minimum Variance Distortionless Response Beamforming (MVDR) algorithm is a kind of adaptive beamforming technology proposed by Capon, which can effectively suppress unwanted signals or interference noises by controlling the output power of array elements to a minimum. At the same time, the beamforming direction of the signal can be correctly received. It can be seen from the model of the received signal of equation (9) is,

$$\boldsymbol{x}_i(t) = s_i(t)\boldsymbol{a}(\theta,\varphi) + \boldsymbol{n}(t) \tag{9}$$

In the process of beamforming, the weighted vector $\boldsymbol{w}$ is searched and the signal $s_0(t)$ is recovered from the array snapshot $x(t)$, i.e.,

$$\boldsymbol{y}_i(t) = s_i(t)\boldsymbol{w}_i^{\boldsymbol{H}}\boldsymbol{a}_i(\theta,\varphi) + \boldsymbol{w}_i^{\boldsymbol{H}}\boldsymbol{n}(t) \tag{10}$$

When $\boldsymbol{w}^H\boldsymbol{a}(\theta)=1$, we can obtain the signal $\boldsymbol{s}(t)$ in (11),

$$\boldsymbol{s}_i(t) = s_i(t) + \boldsymbol{w}_i^H\boldsymbol{n}(t) \tag{11}$$

The mean value of $\boldsymbol{s}_i(t)$ is,

$$E\left[\boldsymbol{s}_i(t)\right] = E\left[s_i(t)\right] + \boldsymbol{w}_i^H E\left[\boldsymbol{n}(t)\right] = s_i(t) \tag{12}$$

It can be seen from the above equation that the estimation of the signal is unbiased when the present equation is established, i.e., $\boldsymbol{w}_i^H\boldsymbol{a}_i(\theta,\varphi)=1$ .Thus the estimated variance is,

$$E\left[\left|\boldsymbol{s}_i(t) - E\left[\boldsymbol{s}_i(t)\right]\right|^2\right] = E\left[\left|\boldsymbol{s}_i(t)\right|^2\right] - \left|s_i(t)\right|^2 \tag{13}$$

According to the estimation theory, the estimation with the minimum variance is the optimal estimation, i.e.,

$$\min E\left[\left|\boldsymbol{s}_i(t) - E\left[\boldsymbol{s}_i(t)\right]\right|^2\right] \tag{14}$$

The above equation is equivalent to,

$$\begin{aligned}\min E\left[\left|\boldsymbol{s}_i(t)\right|^2\right] &= \min E\left[\boldsymbol{w}_i^H\boldsymbol{x}_i(t)\boldsymbol{x}_i^H(t)\boldsymbol{w}_i\right] \\ &= \min \boldsymbol{w}_i^H\boldsymbol{R}_x\boldsymbol{w}_i\end{aligned} \tag{15}$$

The unbiased estimator (13) and the minimum estimator variance (15) of the signal are summarized, i.e.,

$$\begin{cases}\min \boldsymbol{w}_i^H\boldsymbol{R}_x\boldsymbol{w}_i \\ \boldsymbol{w}_i^H\boldsymbol{a}(\theta,\varphi)=1\end{cases} \tag{16}$$

From the above equation, it can be understood that the signal from a certain direction θ can be received correctly, while the useless signal or interference from other directions can be suppressed. The Formula (16) can be solved by Lagrange multipliers to obtain the conditional extremum. Set the target function,

$$L(\boldsymbol{w}) = \frac{1}{2}\boldsymbol{w}^H\boldsymbol{R}_x\,\boldsymbol{w} - \lambda\left[\,\boldsymbol{w}^H\boldsymbol{a}(\theta) - 1\right] \tag{17}$$

So we take the derivative of $\boldsymbol{w}_i$, and we set it equal to 0, and we get the matrix derivative formula,

$$\boldsymbol{R}_x\,\boldsymbol{w} - \lambda\,\boldsymbol{a}(\theta) = 0 \tag{18}$$

Using $\boldsymbol{w}^H\boldsymbol{a}(\theta) = \boldsymbol{a}^H(\theta)\boldsymbol{w} = 1$, i.e.,

$$\lambda = \frac{1}{\boldsymbol{a}^H(\theta)\boldsymbol{R}_x^{-1}\boldsymbol{a}(\theta)} \tag{19}$$

So the optimal weight is,

$$\boldsymbol{w}_{\text{opt}} = \frac{\boldsymbol{R}_x^{-1}\boldsymbol{a}(\theta)}{\boldsymbol{a}^H(\theta)\boldsymbol{R}_x^{-1}\boldsymbol{a}(\theta)} \tag{20}$$

The output power of the array can be obtained,

$$P_i(\theta) = \boldsymbol{w}_i^H{}_{\text{opt}}\boldsymbol{R}_{ix}\boldsymbol{w}_{\text{iopt}} = \frac{1}{\boldsymbol{a}^H(\theta,\varphi)\boldsymbol{R}_{ix}^{-1}\boldsymbol{a}(\theta,\varphi)} \tag{21}$$

In practical application, the power spectrum can be scanned in the whole direction, and the direction corresponding to the peak of the spectral line is the incoming wave direction. The target orientation information obtained by the three sub-arrays also contains the grating lobes due to space undersampling.

III. POCESSING METHODS

Recently, the concept of coprime arrays was introduced as an effective solution for sparse sensing in active and passive scenarios. From the viewpoint of antenna-array theory, the advantages of coprime arrays are related to the fact that the grating lobes of the two sparse arrays are never located at the

same azimuth angle, thanks to the coprimality of the two undersampling factors. Essentially, they can be considered as thinned arrays, for which very high thinning factors can be obtained.

A. Product Processing

To resolve the aliasing ambiguities, the product processor multiplies one sub-array's output with the complex conjugate of the other sub-array's output at each bearing, as is shown in fig.3. The resulting beampattern contains no grating lobes. The product of the processing results obtained is finally taken as the final processing output, that is,

$$P_{proi,j}(\theta,\varphi) = y_i(\theta,\varphi) * conj(y_j^T(\theta,\varphi)), i \neq j \in [1,2,3] \quad (22)$$

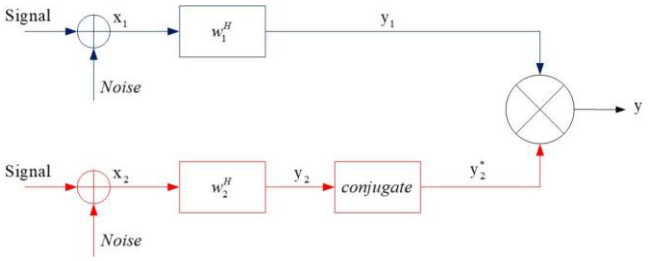

Fig. 3. Product Processing

The resulting product beampattern has no grating lobes, but its highest side lobe is higher than that of ULA. The height of the highest side lobe can be reduced by adding more elements to the sub-arrays to expand the space between the elements [1].

B. Minimum Processing

The processing method selects the minimum value of the scanning response or periodic graph of each subarray at each orientation as its output, as we can see in fig.4, i.e.,

$$P_{\min} = \min(P_{i,j,1}(\theta,\varphi), P_{i,j,2}(\theta,\varphi)) \quad (23)$$

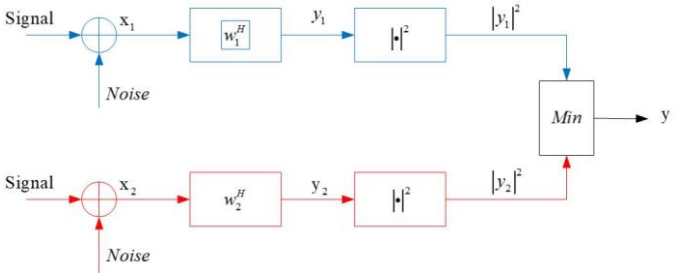

Fig.4. Minimum Processing

Since the periodic graph of the square position array is non-negative, the estimated minimum processing spectrum is guaranteed to be semi-positive regardless of the number of snapshots, and the resulting mininum beampattern does not contain the grating lobes. This detector has the relevant advantage of significantly reducing the side lobe levels with respect to the product detector. The presence of multiple sources can create false peaks in the minimum spectra [2].

C. Comprehensive Processing

In this paper, we combined the product processor and the minimum processor, which inherits the benefits of each of the abovementioned detectors, without the associated drawbacks. In particular, we show that the proposed processing is able to solve critical fake target issues experienced by the min detector in presence of multiple interferes arriving from the grating lobes of both sub-arrays [3], [4], as we can see in (29).

$$P_{\text{com}} = \min(\min(P_{\text{pro1,2}}(\theta,\varphi), P_{\text{pro2,3}}(\theta,\varphi), P_{\text{pro1,3}}(\theta,\varphi)), P_{4ula}) \quad (24)$$

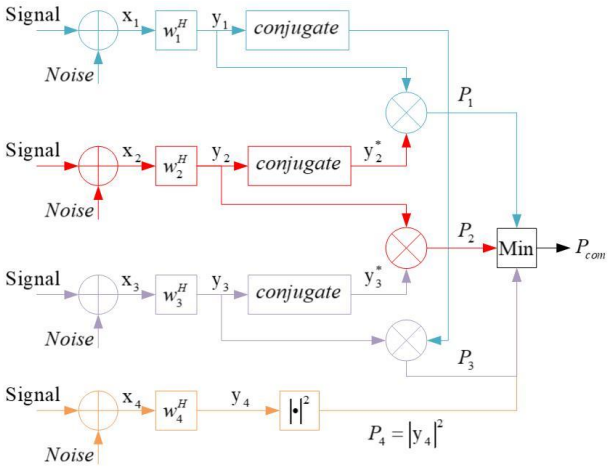

Fig.5. Comprehensive Processing

IV. Simulation Results

In this part, we simulated the tri-parallel array shape and its function, utilizing CBF and MVDR algorithms. We compared the novel array configuration with the common ULA array of half wavelength.

For this part of the simulation, we assume that sub-array I has $C_1 = 3$ sensors, sub-array II has $C_2 = 4$ sensors, and sub-array III has $C_3 = 5$ sensors. The compared ULA has 3 lines, each line has 60 sensors,as it can be seen from Fig. 6.

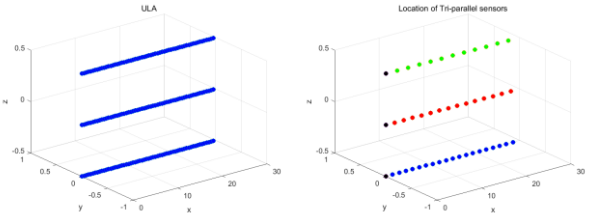

Fig.6. ULA and Tri-parallel array structure

The scanning range is:

Azimuth angle: $\theta \in (0°, 180°)$;

Pitch angle: $\varphi \in (-90°, 90°)$;

Direction of impinging signal: $(\theta_0, \varphi_0) = (90°, 0°)$;

SNR=20dB.

A.ULA

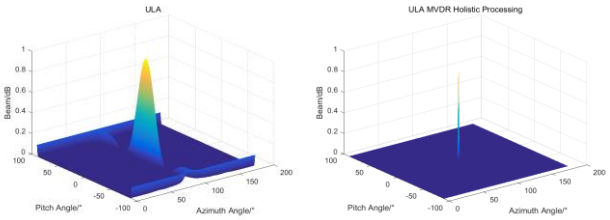

Fig.7. ULA Array Simulation results of CBF, MVDR

B. Tri-Parallel Array

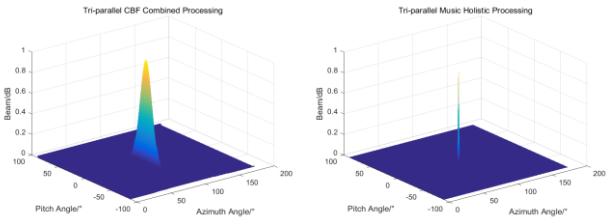

Fig.8.Tri-parallel Array Simulation results of CBF, MVDR

The scanned response obtained with the proposed processor for the above-discussed case, showed in black in Fig.8, testifies that no fake targets are present, similarly to the product detector, and, at the same time, sidelobe levels are never higher than those of the min and product detectors [5].

In fact, in this case, the proposed detector shows both the low sidelobe property of the minimum detector, and the noise rejection property of the product detector.

V. CONCLUSION

In conclusion, the array design and processing in this paper improves the resolution, reduces the complexity of calculation. Achieve large aperture using a novel coprime sparse sensor arrays which receive and process the signal. Compared with the traditional uniform linear array, the proposed array structure has lower computation and higher resolution. Compared with traditional sparse array, the proposed method can estimate the target orientation with higher reliability instead the grating lobes.

REFERENCES

[1] Yang Liu, John R. Buck, “Gaussian Source Detection and Spatial Spectral Estimation Using a Coprime Sensor Array With the Min Processor”, IEEE TRANSACTIONS ON SIGNAL PROCESSING, VOL. 66, NO. 1, JANUARY 1, 2018.

[2] Gerardo Di Martino, Antonio Iodice, “Passive beamforming with coprime arrays”, IET Radar Sonar Navig., 2017, Vol. 11 Iss. 6, pp. 964-971.

[3] Yang Hu, Yimin Liu and Xiqin Wang, “DOA Estimation of Coherent Signals on Coprime Arrays Exploiting Fourth-Order Cumulants”, Sensors 2017, 17, 682; doi:10.3390/s17040682.

[4] Y. Liu, John R. Buck, “High-resolution DOA Estimation In SNR and Snapshot Challenged Scenarios using Multi-frequency Co-prime Arrays”, Computer Engineering Department, University of Massachusetts Dartmouth.

[5] Sheng Liu, Lisheng Yang, Dong Li, Hailin Cao and Qingping Jiang, “2D DOA estimation for noncircular sources using L-shaped sparse array”, Multidim Syst Sign Process (2018) 29:489–502.